J. Membrane Biol. 95, 241–254 (1987)

The Journal of
Membrane Biology

Cell Membrane and Transepithelial Voltages and Resistances in Isolated Rat Hepatocyte Couplets

J. Graf‡†, R.M. Henderson§‡, B. Krumpholz†, and J.L. Boyer‡
Departments of §Physiology and ‡Medicine, Liver Center, Yale University School of Medicine, New Haven, Connecticut 06510, and †Department of General and Experimental Pathology, University of Vienna, A-1090 Vienna, Austria

Summary. The basic electrical properties of an isolated rat hepatocyte couplet (IRHC) system have been analyzed using classical techniques of epithelial electrophysiology, including measurement of electric potentials, resistances and intracellular ion activities. Applications of these techniques are discussed with respect to their limitations in small isolated cells. Mean intracellular and intracanalicular membrane potentials ranged from −23.7 to −46.7 and −4.3 to −5.9 mV, respectively. Membrane resistances were determined using an equivalent circuit analysis modified according to the geometry of the IRHC system. Resistances of the sinusoidal (basolateral) and canalicular (luminal) cell membranes and tight junctions averaged 0.15 and 0.78 GΩ and 25 MΩ, respectively. The cells are electrically coupled via low resistance intercellular communications (~58 MΩ). Intracellular ion activities for Na^+, K^+ and Cl^- averaged 12.2, 88.1 and 17.7 mmol/liter, respectively. The basolateral membrane potential reveals a permeability sequence of $P_K > P_{Cl} > P_{Na}$. The luminal potential showed minimal dependence on changes in transjunctional ion gradients, indicating a poor ion selectivity of the paracellular pathway. The electrogenic (Na^+-K^+)-ATPase contributes little to the luminal and cellular negative electric potential. Therefore, the luminal potential probably results from the secretion of impermeant ions and a Donnan distribution of permeant ions, a mechanism which provides the osmotic driving force for bile formation. By providing the unique opportunity to measure luminal potentials, this isolated hepatocyte system permits study of secretory mechanisms for the first time in a mammalian gland using electrophysiologic techniques.

Key Words hepatocyte · ion conductances · membrane potential · (Na^+/K^+)-ATPase · intracellular ion activities · sinusoidal membrane · canalicular membranes · paracellular transport

Introduction

Electrophysiologic approaches have elucidated the mechanisms for solute and water transport across many epithelial tissues. Such studies of the liver have been limited to recordings of intracellular potentials in whole organ and isolated hepatocytes. These studies have addressed questions such as ion permeabilities of the cell membrane, primary and secondary electrogenic transport processes and the effects of hormones on these parameters. However, electrophysiologic studies of the bile secretory process in the liver have not been possible because of anatomical constraints that preclude direct access to the bile canalicular lumen. Recently we have developed an isolated liver cell system that enables direct measurements of intraluminal (canalicular) potentials, suggesting that classic electrophysiologic techniques can be applied to the study of bile secretory mechanisms (Graf, Gautam & Boyer, 1984).

Following collagenase perfusion of rat liver, hepatocytes can be identified that retain junctional contacts with adjacent cells. When placed in short-term culture, selected hepatocyte couplets reseal these junctional contacts to form a closed canalicular space. During several hours in culture the space expands as secretion takes place. As previously described by this laboratory, many of the secretory properties of this isolated cell couplet system are similar to the bile secretory process in intact liver tissue (Graf et al., 1984). This secretory unit retains the ability to transport fluorescein from the medium into the canalicular lumen. The tight junctions of the couplets exclude Ruthenium red (Boyer, Ng & Gautam, 1985) and the canaliculi both expand in response to bile acids and shrink following addition of sucrose to the media, changes that respectively correspond to stimulation and inhibition of bile secretion in the intact organ. However, in contrast to the intact liver, the secretory products remain within the canalicular space until the lumen either spontaneously contracts or collapses due to disruption of the junctional complexes as secretory pres-

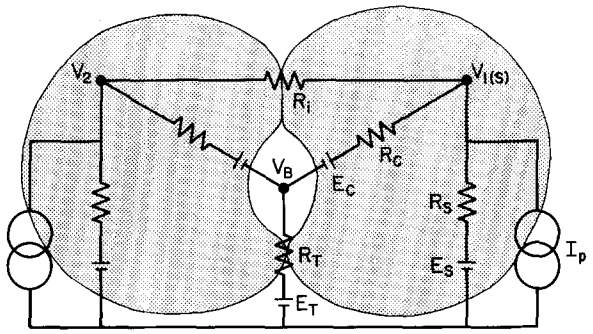

Fig. 1. Equivalent circuit of IRHC. The diagram shows the electromotive forces (E), current source (I) and the resistive elements (R) that may be responsible for generation of the electric potential gradients (V, with reference to bath) recorded in the IRHC. At the sinusoidal and canalicular membrane and tight junction (subscripts S, C, T, respectively), the voltage difference (V_S, $V_C = V_S - V_B$, respectively) may result from the electromotive forces at these barriers (diffusion potentials, E_S, E_C and E_T). In addition, current generation by all the emf's or an electrogenic ion pump at the basolateral membrane (I_p) would result in an IR drop across their resistors (R_S, R_C, R_T). The analysis given in the text indicates that in the IRHC individual emf's are the main source of the respective voltage differences with little contribution of current flowing in the loop (R_S, R_C, R_T) or current produced by the ion pump. The presence of R_i in the circuit shows that cells are electrically coupled by low resistance intercellular communications

sure rises. In the meantime, during expansion of the canalicular space, micropipettes can be placed within the lumen so that, besides intracellular, intraluminal (transepithelial) potential measurements can be obtained.

In the present study we explore the basic electrophysiological properties of this isolated cell system in order to analyze the determinants of these potential gradients by measuring: (i) the resistances of the transcellular and paracellular pathways, (ii) intracellular ion activities of sodium, potassium, and chloride, (iii) the effects of changes of external concentrations of sodium, chloride and potassium on intracellular and intracanalicular potentials, and (iv) the effect of ouabain inhibition and potassium reactivation of the sodium pump on intracanalicular and intracellular potentials.

Materials and Methods

Isolated rat hepatocytes were prepared and characterized according to Seglen (1976) as modified in this laboratory (Blitzer et al., 1982; Graf et al., 1984). Cells were suspended in Liebovitz-15 tissue culture medium (Gibco; $\sim 10^5$ cells/ml), placed in an incubator at 37°C in an air atmosphere and allowed to settle onto 5 × 5 mm glass coverslips until studied 3–8 hr after isolation.

The optical and electrical set up was essentially as described (Graf et al., 1984). It consists of a Zeiss IM35 inverted microscope, placed on a vibration-free table and housed in a Faraday cage. Double differential interference contrast optics were used (objective: Neofluar 63/1.26). A coarse and a fine, hydraulic drive micromanipulator (Narishige, Tokyo) were mounted on either side of the microscope stage, to allow puncturing of cells at an angle of ~30°. Cells were either studied in L-15 culture medium as described (*see* Results, section I) or under continuous superfusion with bicarbonate-buffer (for composition, *see below*). Superfusion was from reservoirs by gravity at a rate of 5 ml/min. Three solutions were pre-equilibrated with 5% CO_2, 95% O_2. Immediately before entering the bath, the three lines passed through a Perspex box, where 3 × 1.5 m lengths of Silastic tubing were coiled around a cylinder made of a metal grid, heated to 37°C by an axial resistor. The solutions were again equilibrated through the tubing wall with humidified CO_2/O_2. This system allowed rapid changes of fluid flow through either of the three lines into the chamber (volume 0.5 ml) with negligible temperature transients (<1°C).

The electrical equipment consisted of an FD223 amplifier and a 7071A amplifier in a 7100A mainframe, an Anapulse 30-1 T stimulator and a stimulus isolation unit (all WPI, New Haven, CT), a Tektronix RM5-2A oscilloscope and two Gould 220 pen recorders. For input resistance measurements rectangular current pulses were passed through the potential recording electrode. The resistance and capacitance of the microelectrode was compensated by a bridge circuit. Proper electrode resistance compensation is critical and measurements were not accepted if the electrode resistance changed after an impalement or if a short time constant of the voltage change was apparent during intracellular recording.

Microelectrodes were pulled from Omega dot borosilicate glass tubing (Frederick Haer & Co, Brunswick, Maine) (OD/ID 1.2/0.6 or 1.0/0.5 mM) on a Narishige PD5 horizontal puller to have resistances of about 150 MΩ when filled with 1 M KCl.

Double-barreled electrodes were constructed by aligning two 7-cm pieces of thick wall borosilicate glass tubing in parallel in the heating loop of a Narishige PD5 puller. Two 2-mm o-rings cut from heat-shrink tubing, were placed 1 cm to the left and right of the loop around the pieces of glass tubing. By turning on the heat the o-rings shrank and firmly held the glass together which was then twisted by approximately 240°. Electrodes were pulled so that each barrel had about 120 MΩ resistance when filled with 1 M KCl. Electrodes were silanized by exposure to hexamethyldisilazane vapor (Fluka, Buchs, Switzerland). The following liquid ion exchangers (LIX) were used: K^+: IE 190 (WPI); Cl^-: chloride micro exchanger 477913 (Corning); Na^+: IE 110 (WPI). Reference barrels were filled with 2% potassium-tetrakis-*p*-chlorophenyl borate in octanol (Thomas & Cohen, 1981). Using a second KCl-filled microelectrode as a control in the same cell these LIX-reference electrodes revealed similar potential readings (within 2 mV). In some experiments measurements of intracellular ion activities were also performed with two single barrelled microelectrodes, one containing the ion selective, the other the reference LIX.

The performance of ion selective electrodes (slope, ability to penetrate cells) was considerably improved by manual tip bevelling (Henderson, Graf & Boyer, 1987). Na^+ and K^+ microelectrodes were calibrated in mixtures of 150 mM NaCl and 150 mM KCl at constant ionic strength. K^+ electrodes exhibited a slope of >55 mV/decade; Na^+ electrodes were used when their slope was >40 mV/decade. Cl^- electrodes were calibrated in NaCl/Na-gluconate mixtures and had slopes of >50 mV/decade.

Calculations

In accordance with the equivalent circuit in Fig. 1, a set of equations has been used to derive the parameters reported in the text. This circuit is analogous to models applied in epithelial electrophysiology (e.g. Boulpaep & Sackin, 1979; Graf & Giebisch, 1979) taking into account the particular geometry of the IRHC. In this model two epithelial cells enclose a luminal space which is surrounded by a circular tight junction at the cell contacts and thus this space is sealed off from the bathing medium. The circuit also includes a basolateral electrogenic pump depicted as a current source with infinite internal resistance.

Table of Symbols Used

V_S	Intracellular electric potential with reference to bath
V_1 & V_2	Intracellular electric potential recorded in the right hand and left hand cell of Fig. 1 when two electrodes were used
V_B	Intraluminal biliary electric potential with reference to bath
V_C	Canalicular membrane potential ($V_C = V_S - V_B$)
R_S, R_C	Sinusoidal (basolateral) and canalicular (luminal) membrane resistance of a single cell
B	Voltage divider ratio $B = R_C/R_S$
R_T & R_i	Resistance of the tight junction (paracellular pathway) and intercellular communications (gap junctions) of the couplet
E_S, E_C, E_T	Electromotive forces at the sinusoidal, canalicular, and tight junction barriers
I_p	Pump current produced at the basolateral membrane of a single cell
I_L	Current in the loop $R_S - R_T - R_C$ for a single cell generated by the emf's at these barriers
I_1	Current injected into cell 1, voltage changes (V^1) produced by this current are marked with superscript 1
I_B	Current injected into lumen, voltage changes (V^B) produced by this current are marked by superscript B.
R_B	Canalicular input resistance
R_1	Cellular input resistance

Equations used

$$V_B = \frac{E_T(R_S + R_C) + 2R_T(E_S - E_C) - 2I_pR_TR_S}{R_S + 2R_T + R_C} \quad (1)$$

$$V_S = \frac{E_S(2R_T + R_C) + R_S(E_T + E_C) - I_p(R_C + 2R_T)R_S}{R_S + 2R_T + R_C} \quad (2)$$

$$E_S = \frac{2R_TV_S + R_S(V_B - E_T)}{2R_T} \quad (3)$$

$$E_C = \frac{2R_T(V_S - V_B) + R_C(E_T - V_B)}{2R_T} \quad (4)$$

$$I_L = \frac{E_S - E_T - E_C}{R_S + 2R_T + R_C} \quad (5)$$

$$R_B = V_B^B/I_B = \frac{R_T(R_C + R_S)}{2R_T + R_C + R_S} \quad (6)$$

$$B = \frac{\Delta V_B^B - \Delta V_2^B}{\Delta V_2^B} = \frac{R_C}{R_S} \quad (7)$$

$$R_S = \frac{(B + 1)^2(\Delta V_1^1 + \Delta V_2^1) - 2I_1R_B}{I_1^B(B + 1)} \quad (8)$$

$$R_T = \frac{R_BR_S(B + 1)}{R_S(B + 1) - 2R_B} \quad (9)$$

$$R_i = \frac{R_SR_C(\Delta V_1^1 - \Delta V_2^1)}{\Delta V_2^1(R_S + R_C) - R_T(I_1R_S - \Delta V_1^1 - \Delta V_2^1)} \quad (10)$$

$$R_1 = \Delta V_1^1/I_1 = \frac{R_S[R_SR_i(R_T + R_C) + R_C(R_S + R_i)(R_C + 2R_T)]}{(2R_T + R_S + R_C)[2R_SR_C + R_i(R_S + R_C)]} \quad (11)$$

To obtain estimates of changes of R_S and R_T in ion substitution experiments we recorded the input resistances R_1 and R_B. Assuming that R_C and R_i do not change and combining Eqs. (6) and (11) by eliminating R_T gave a cubical equation solved for R_S. From this R_T was calculated using Eq. (6).

Electrolyte Solutions

Control solutions for superfusion of isolated cells contained 115 mM NaCl, 5 mM KCl, 25 mM $NaHCO_3$, 2 mM NaH_2PO_4, 1 mM $MgSO_4$, 2 mM $CaCl_2$, 1 mM Na pyruvate and 5 mM D-glucose. In ion replacement studies the osmolarity was kept constant, K^+ was increased, replacing Na^+, and Na^+ and Cl^- was varied by replacement with organic ions to obtain the concentrations given in Table 3 (Na^+ and Cl^- were replaced with N-Methyl-D-glucamine and isethionic acid, respectively, Sigma, St. Louis, MO).

All data are given as mean ± SEM (n = number of observations).

Results

I. Measurements of Resistances of Basolateral and Canalicular Cell Membrane Domains and of Intracellular Communications and Tight Junctions

To obtain measurements of the resistive elements of the equivalent circuit shown in Fig. 1, we made use of techniques previously applied to determine resistances of the luminal (apical) and basolateral cell membranes, tight junctions and intracellular communications in classical transporting epithelia (Boulpaep & Sackin, 1979; Graf & Giebisch, 1979). By analogy, the transepithelial resistance was determined as the bile canalicular input resistance (R_B), i.e., the total resistance for current flow

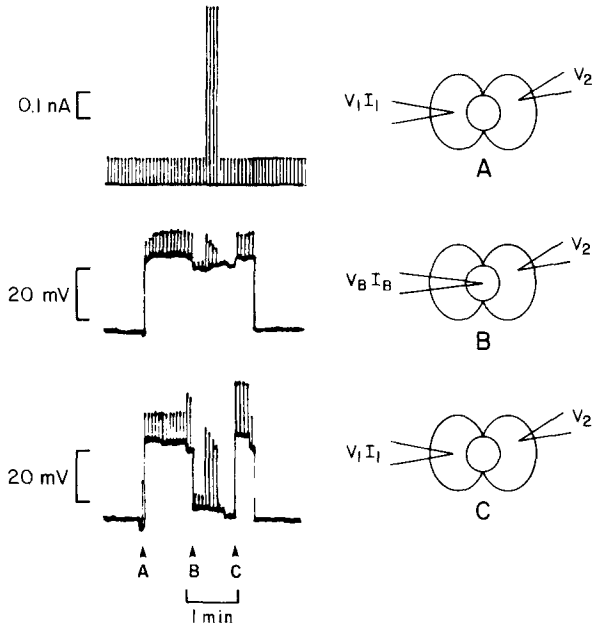

Fig. 2. Determination of the resistive elements of the equivalent circuit in Fig. 1 using two microelectrodes. The positions of the two microelectrodes in the couplet during the course of the experiment are shown in the diagrams on the left (*A*, *B* and *C*, corresponding to arrows *A*, *B* and *C* below bottom trace). *Lower trace:* potential trace of the first electrode through which current pulses were passed after extracellular electrode resistance compensation (measuring V_1 and V_B). *Middle trace*: potential trace of the second electrode inserted into cell 2 (measuring V_2). *Upper trace*: amplitude of current pulses (*I*) passed through electrode 1. At the left arrow (*A*, below bottom trace) both electrodes were inserted simultaneously into the two cells measuring V_1 and V_2, respectively, as well as their electrotonic changes due to current injection into cell 1. This reveals the intracellular input resistance ($\Delta V_1/I_1$) and the cell coupling ratio ($\Delta V_2/\Delta V_1$). At the middle arrow (*B*) electrode 1 was inserted into the canalicular lumen measuring V_B. In this electrode configuration the intracanalicular input resistance ($\Delta V_B/I_B$) and the voltage divider ratio ($\Delta V_2^B/(\Delta V_2^B + \Delta V_B^B)$) were obtained at low and high current amplitudes. At the third arrow (*C*) electrode 1 was retracted into cell 1 and, thereafter, both electrodes were withdrawn simultaneously. (Vertical lines between potential trace and the electrotonic deflections are drawn by hand—thermo-pen recording). (Negative potentials are shown by upward deflection)[1]

(I_B) out of the canalicular lumen by the paracellular route, the tight junction resistance (R_T) and the transcellular route, the resistance of the canalicular (R_C), and basolateral sinusoidal (R_S), cell membranes, respectively. A second electrode was simultaneously inserted into one of the two hepatocytes. As current was passed into the lumen this intracellular electrode measured the voltage change between the series resistors R_C and R_S revealing the voltage divider ratio $\Delta V_2^B/\Delta V_B^B$. Alternatively, current was passed into one cell (Claret, Coraboeuf & Favier, 1970). The resulting voltage change in this cell (ΔV_1) defines the cellular input resistance (R_1), i.e., the resistance for current flow out of this cell through R_S, R_C and the intercellular communication via gap junctions (R_i), R_1 being a composite of all the resistances of the circuit. Voltage changes in the second cell (ΔV_2) were recorded while current was passed into the first cell. ΔV_2 depends on the magnitude of the coupling resistance R_i and of the resistances for current flow out of the second cell into the bathing media, thus defining the coupling ratio, ($\Delta V_2/\Delta V_1$; Loewenstein, 1979). Measuring R_B, R_1, $\Delta V_2^B/\Delta V_B^B$ and $\Delta V_2^1/\Delta V_1^1$ therefore permits calculation of R_S, R_C, R_T and R_i using the equations given in Materials and Methods. Figure 2 shows an experiment where these parameters were measured. Data from 20 such experiments are summarized in Table 1. Rough estimates of specific membrane conductances (g_S, g_C) and conductances for unit tight junctional length (g_t) are also included in Table 1 and were obtained by measuring cellular and luminal diameters, assuming these structures to be spherical and calculating surface areas and luminal circumference, respectively. These estimates ignore surface area enlargement by membrane invaginations and microvilli which increase membrane area in intact liver by a factor of 3 (Weibel et al., 1969). The true values of specific membrane conductances might therefore be overestimated in these isolated cell preparations.

As illustrated in Fig. 1 the potential gradients across the luminal (V_C), basolateral (V_S) and tight junction barriers (V_B) are determined by two components: their individual electromotive forces (E_C, E_S, E_T) and the current (I_L) flowing through their

[1] Traces in Fig. 2 show a series of typical artifacts: (i) Before insertion into cell 1, electrode 1 shows a depolarization and a large input resistance (ΔV_1 amplitude of electrotonic potential deflections) as the electrode tip touches the cell membrane. (ii) After insertion into cell 2 (at *A*), electrode 2 shows a slow increase of the membrane potential in both cells. V_2 also increases, indicating "sealing in" of electrode 2. (iii) Before insertion into the lumen ΔV_1 is large as the electrode 1 touches the luminal membrane from inside the cell. (iv) After insertion of the electrode 1 into the lumen (at *B*), V_2 is slightly depolarized, most likely due to a leak reducing R_C. (v) Immediately after increasing the amplitude of current pulses (upper trace) delivered into the lumen, the lumen started to collapse. This event is reflected by the decrease of V_B and V_B in lower trace and the reduction and disappearance of ΔV_2 as all current leaves the lumen via the paracellular route, presumably due to opening of tight junctions during collapse. (vi) Upon withdrawal of electrode 1 into cell 1 the electrode resistance was no longer compensated (large ΔV_1, lower trace). Traces showing artifacts i, ii, iii and vi were accepted, those showing artifact iv only if V_2 depolarized by <5 mV and those showing example v only when a stable reading was obtained prior to a collapse of the lumen.

resistances R_C, R_S and R_T, respectively (e.g. $V_C = E_C - I_L R_C$). The amount of current in the loop $R_C \rightarrow R_S \rightarrow R_T$ had been determined in isolated preparations of other transporting epithelia, where the composition of bathing media on both sides of the epithelium could be experimentally controlled (Boulpaep & Sackin, 1979), thus allowing estimates of the electromotive forces. One condition frequently applied is to use identical bathing solutions, thus setting $E_T \sim 0$ where $I_L R_T$ alone defines the transepithelial potential (equivalent to V_B). The corresponding values, E_C and E_S, can then be determined. The condition where $E_T = 0$ may not be applicable to the IRHC, and data in intact liver rather indicate a Donnan distribution between bile and blood (Graf, 1983) where $E_T = V_B$ and $I_B = 0$. In the latter case $V_S = E_S$ and $V_C = E_C$, whereas for $E_T = 0$, $I_L = 87$ pA, $E_S = -41.7$ mV and $E_C = +43.8$ mV.

Table 1. Electrical data from IRHC

V_1	−28.3	±	1.9 mV
V_2	−27.9	±	1.7 mV
V_B	−4.3	±	0.6 mV
$V_B^B/I_B = R_B$	26.8	±	3.3 MΩ
V_2^B/I_B	5.6	±	1.1 MΩ
V_2^B/V_B^B	0.20	±	0.02
$V_1^l/I^l = R_l$	73.5	±	4.4 MΩ
V_2^l/I_l	52.8	±	3.4 MΩ
V_2^l/V_1^l	0.73	±	0.03
Cell surface area	2153	±	91 μm^2
Luminal surface	95	±	15 μm^2
Luminal circumference	16.5	±	1.6 μm
R_S	153.7	±	9.7 MΩ
R_C	778.5	±	78.4 MΩ
R_T	24.7	±	2.9 MΩ
R_i	58.3	±	11.3 MΩ
g_S	328	±	18 $\mu S/cm^2$
g_C	4488	±	660 $\mu S/cm^2$
g_t	37.1	±	4.9 $\mu S/cm$

II. Intracellular Ion Activities

Intracellular ion activities were determined, using double-barreled or two single-barreled microelectrodes. One barrel recorded the intracellular electric potential (V_S) the other was filled with ion selective resin and recorded $V_S - E_i$ upon impalement (E_i = transmembrane ion potential gradient). Although the dimensions of each of the two barrels of the double-barreled electrodes were similar to conventional Ling-Gerard electrodes (> 100 MΩ), membrane potential readings were often lower than those obtained with single-barrel electrodes. Impalements with potential readings of $V_S < -20$ mV were discarded. The data obtained are summarized in Table 2 in which C_i and C_o are, respectively, the intracellular and extracellular ion concentrations and a_i the intracellular ion activity calculated using an activity coefficient of 0.756.

It should be emphasized that, although only impalements with stable potential readings were accepted, the value of E_{Cl} usually decreased after impalement, whereas E_{Na} and E_K remained unaltered. The rate of decrease of E_{Cl} appeared to be related to the magnitude of $V_S - E_{Cl}$, suggesting conductive Cl^- influx until electrochemical equilibrium was attained after 2 to 4 min where $V_S \simeq E_{Cl}$. These steady-state values are plotted in Fig. 3. Further evidence for the equilibrium distribution of Cl^- is shown in Fig. 4. One cell of the couplet was impaled with a Ling-Gerard type microelectrode, filled with 0.5 M K_2SO_4 and the other cell with a double-barreled Cl^--sensitive microelectrode. D.C. current was passed through the Ling-Gerard electrode which led, by current flow through the intercellular communication, to a change in V_S in the partner cell. As V_S was changed so the intracellular Cl^- activity changed in accordance with a passive transmembrane distribution of Cl^-. For further details *see* legend.

III. Effect of Ion Replacement on Intracellular and Intraluminal Electric Potential and Input Resistances

The electric potential difference across a membrane is described by $V_m = t_i E_i + I/g_m$ where $t_i = g_i/g_m$, t_i = transference number for an individual ion, g_i = partial ionic membrane conductance, g_m = total membrane conductance, E_i = transmembrane ion potential difference, $E_i = RT/F \times \ln [i]_{ext}/[i]_{int}$ (Nernst potential) and I = electrogenic pump current). In order to obtain estimates of the ion conductances of the tight junctions and the sinusoidal cell membrane, changes in the intracellular and intraluminal electric potential (ΔV_S, ΔV_B) and input resistances (ΔR_1, ΔR_B) were measured with single electrodes while ion concentrations in the bathing media were varied (ΔE_i). Sodium concentrations were reduced by equimolar replacement with K^+ or the less permeant ion N-methyl-D-glucamine (NMG). Cl^- concentration was reduced by replacement with isethionate (IE).

Examples of these ion substitution experiments are illustrated in Fig. 5, and data are summarized in Table 3. When external K^+ was increased at the expense of Na^+, the cells depolarized (ΔV_S) and resistance to current flow out of the cells (R_1) also

Table 2. Measurement of intracellular ion activities in IRHC

Ion	Number of measurement	V_m (mV)	C_i (mmol/liter)	C_o (mmol/liter)	a_i (mmol/liter)	E_i (mV)
Na^+	9	−23.7 ± 1.8	16.3 ± 0.9	143.0	12.2	+57.9 ± 1.4
K^+	20	−25.1 ± 1.1	117 ± 3.2	5.0	88.1	−83.5 ± 0.7
Cl^-	19	−31.5 ± 2.0	23.6 ± 1.1	124.0	17.7	−44.3 ± 2.0

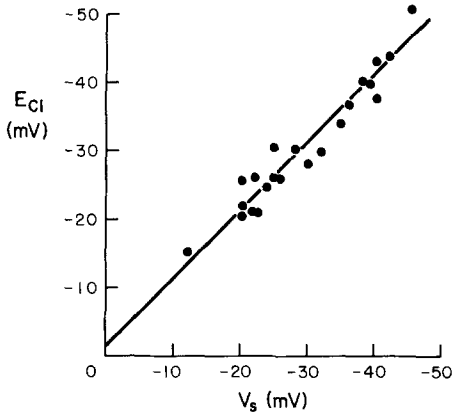

Fig. 3. Dependences of E_{Cl} (measured in mV) on the intracellular electric potential. Steady-state recordings of E_{Cl} are plotted against the sinusoidal membrane potential (V_S). The correlation ($E_{Cl} = 1.03 \times V_S + 1.34$ mV, $r = 0.97$) indicates that Cl^- is passively distributed across the sinusoidal membrane barrier where $V_S - E_{Cl} = 0$

decreased simultaneously. Both of these observations indicate a relatively high membrane K^+ conductance. In contrast, relatively small changes in the luminal potential (ΔV_B) and input resistance (R_B) were observed, indicating that the paracellular pathway exhibits little discrimination between Na^+ and K^+.

Reducing external Na^+ by partial replacement with NMG hyperpolarized both the cellular and luminal potential. The increase in input resistance was proportionally larger in the lumen than in the cell, indicating a relatively high Na^+ conductance of the paracellular pathway compared to the basolateral cell membrane.

Partial replacement of Cl^- by IE reduced the cellular and luminal potential, and this was also associated with a significant increase of both cellular and luminal input resistances. These findings are consistent with a relatively high Cl^- conductance across both the paracellular pathway and basolateral cell membrane.

Table 4 gives results of calculations of changes of the emf at the sinusoidal membrane (ΔE_S) and tight junctional barriers (ΔE_T) and of the specific resistances (R_S and R_T) during ionic shifts. (*see* Materials and Methods). These estimates were based on the assumption that the canalicular membrane resistance (R_C), the coupling resistance (R_i) as estimated above (Table 1), and the emf at the canalicular membrane (E_C) did not change initially as an immediate result of changes in the external solutions. However, replacement of Na^+ and Cl^- with the less permeant solutes (NMG, IE) led to rapid shrinkage of the luminal spaces, suggesting that ion concentrations within this space actually may have changed and thus R_C and E_C may have been altered.

IV. Effects of Ouabain, K^+-Deprivation and K^+-Readmission

To determine the contribution of Na^+, K^+-ATPase to the intracellular and intraluminal electric potentials, we studied the effects of inhibition and activation of this ion pump. Ouabain (1 mM) was used to inhibit the pump, and activation was achieved by readmission of K^+ after the cells were first allowed to lose K^+ (and gain Na^+) in K^+-free medium (Graf & Petersen, 1978).

Ouabain caused an initial small-step depolarization of the cells (2.9 ± 0.7 mV) within 30 sec followed by a slower progressive decrease of the membrane potential. This depolarization was reversible upon removal of ouabain. In contrast, ouabain did not produce a significant step change in the luminal potential, although a slow depolarization occurred which was also reversible after the inhibitor was removed (Fig. 6).

In order to activate the Na pump, cells were first placed in K^+-free medium for at least 45 min and then transferred to the microscope perfusion chamber where they were continuously superfused with K^+-free medium. These K^+ deprived cells were then impaled either with single-barreled or with double-barreled K^+-sensitive microelectrodes. The period of K^+ deprivation ranged from 45 to 90 min, and within this period of K^+-free incubation

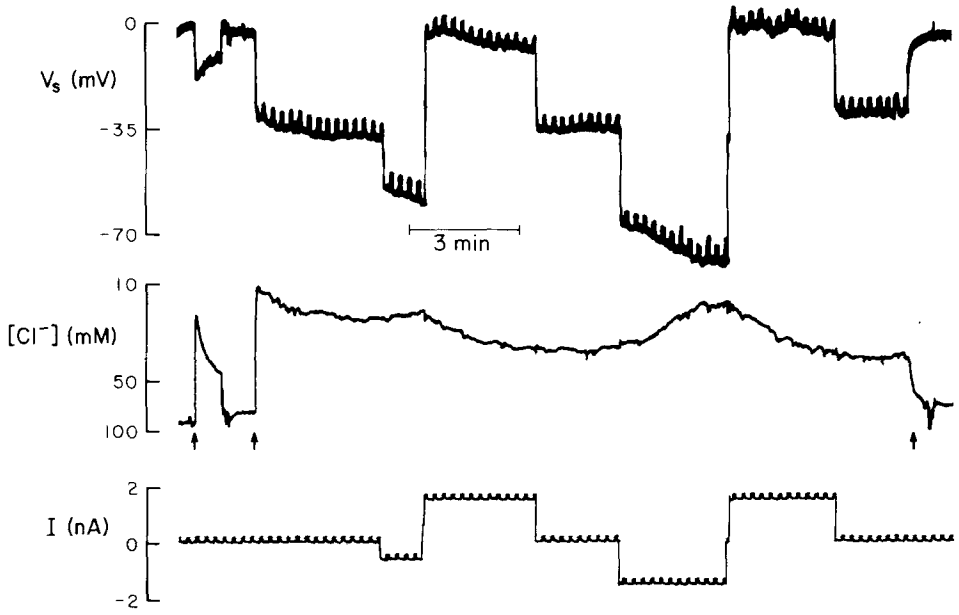

Fig. 4. Dependence of internal chloride concentration on the sinusoidal membrane potential (V_S) under current clamp conditions. One cell of the couplet was impaled with a 0.5 M K_2SO_4-filled microelectrode through which DC current of different sign and amplitude was passed (I). Current flow through the intercellular communication leads to a voltage change in the second cell. This second cell was impaled with a double barreled microelectrode, one barrel recording the intracellular potential (V_S), the other $V_S - E_{Cl}$, giving the differential trace E_{Cl} calibrated to show log $[Cl^-]_i$. Note that immediately after impalement $[Cl^-]_i$ slightly increases to a level where $V_S - E_{Cl} = \approx 0$. This state is also attained when V_S is varied by the clamp current. This is shown by the decrease of $[Cl^-]_i$ following hyperpolarization of V_S and increase of $[Cl^-]_i$ upon depolarization (one of five similar experiments is shown). Arrows below middle trace: first arrow, unsuccessful impalement; second arrow, successful impalement; third arrow, electrodes withdrawn

internal K^+ concentration decreased to 31.0 ± 5.7 mmol/liter (n = 11) and cells were depolarized to −12.8 ± 0.8 mV (n = 19).[2] Within 30 sec of K^+ readmission (10 mM) the membrane potential was hyperpolarized by −8.7 ± 0.6 mV and $[K^+]_i$ measured after 1 min was 40.4 ± 6.3 mmol/liter (ΔV_S = 9.4 ± 1.0). A typical trace of the change in mem-

[2] In two instances the gain of internal Na^+ was measured after shifting cells to K-free medium. Intracellular Na^+ concentration rose from 9.8 to 12.4 and from 22 to 27 mmol/liter within the first minute.

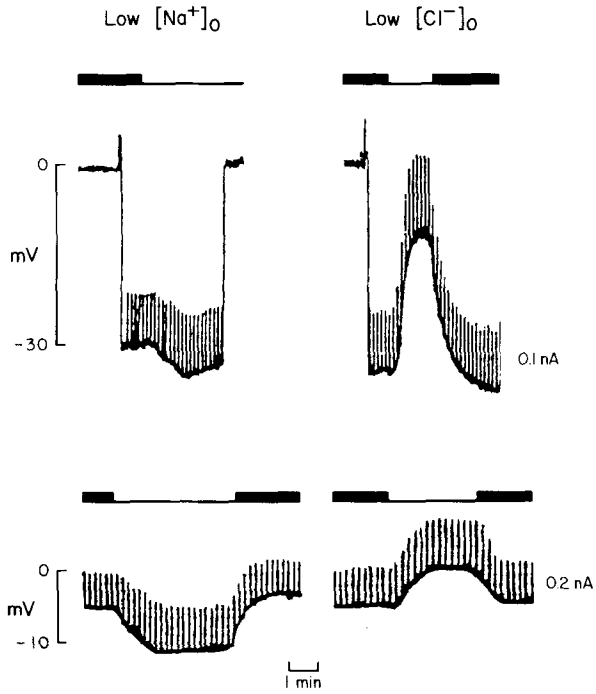

Fig. 5. Effects of ion replacement on the intracellular (V_S) (upper traces) and intraluminal (V_B) (lower traces) electric potential and the respective input resistances R_i and R_B. Input resistances are reflected by the amplitude of the multiple electrotonic potential deflections set up by 100-msec current pulses passed through the recording electrode. Examples are: replacement of Na^+ by N-methyl-D-glucamine (left-hand traces) and of Cl^- by isethionate (right-hand traces). Sodium was reduced from 143 to 3 mM and chloride from 124 to 4 mM

Table 3. Changes of intracellular and intracanalicular electrical potentials and input resistances in ion substitution experiments

	Concentration (mM)	N	V_s (mV)	R_i (MΩ)	N	V_B (mV)	R_B (MΩ)
1) Low sodium							
Control	Na^+: 143	16	−37.8 ± 1.5	111.6 ± 10.3	8	−5.1 ± 0.7	34.4 ± 3.0
NMG	Na^+: 3		−43.1 ± 1.5	127.5 ± 10.8		−9.4 ± 1.0	50.6 ± 4.2
Difference			−5.3 ± 0.5	15.9 ± 2.2		−4.3 ± 0.4	16.3 ± 1.7
2) High Potassium							
a) Control	Na^+: 143, K^+: 5	10	−43.1 ± 1.4	106.5 ± 5.8	6	−4.3 ± 0.4	25.8 ± 4.1
20 K	Na^+: 128, K^+: 20		−31.7 ± 1.5	73.5 ± 5.8		−1.8 ± 0.4	24.2 ± 4.1
Difference			9.7 ± 1.3	33.0 ± 1.6		2.5 ± 0.2	1.7 ± 1.2 (NS)
b) Control	Na^+: 143, K^+: 5	10	−46.7 ± 2.0	87.5 ± 8.2	8	−5.9 ± 0.7	21.9 ± 1.8
50 K	Na^+: 98, K^+: 50		−20.5 ± 1.3	38.1 ± 3.3		−2.3 ± 0.5	17.5 ± 1.2
Difference			26.2 ± 1.5	49.5 ± 6.7		3.6 ± 0.4	4.4 ± 1.6 (*)
c) Control	Na^+: 143, K^+: 5	12	−44.8 ± 1.6	89.2 ± 4.0	11	−4.6 ± 0.7	29.9 ± 4.2
100 K	Na^+: 48, K^+: 100		−7.9 ± 0.8	38.8 ± 1.9		0.1 ± 0.5	15.9 ± 2.2
Difference			36.8 ± 1.6	50.4 ± 2.8		4.7 ± 0.4	14.1 ± 2.2
3) Low Chloride							
Control	Cl^-: 124	14	−35.7 ± 1.6	84.6 ± 6.5	9	−4.8 ± 1.0	24.4 ± 4.0
IE	Cl^-: 4		−17.0 ± 1.4	107.9 ± 7.3		−0.9 ± 1.3	37.2 ± 4.6
Difference			18.7 ± 1.5	23.3 ± 3.0		3.9 ± 0.4	12.8 ± 3.0

Values were obtained immediately before and 30 sec after the ionic shift (*compare* Fig. 5). The respective control and experimental data were significantly different ($P < 0.01$, t test of paired data) except those marked NS (not significant) and * ($0.05 > P > 0.01$).

Table 4. Calculated changes of the electromotive forces and resistances across the sinusoidal cell membrane and tight junctions in ion substitution experiments

	ΔE_i (mV)	E_S (mV)	R_S (MΩ)	E_T (mV)	R_T (MΩ)
Low sodium					
Control		−37.8	257.6	−5.1	36.8
NMG	ΔE_{Na}: −102.4	−43.5	308.8	−9.2	55.8
ΔE		−5.7		−4.1	
R exp/R contr			1.20		1.52
High potassium					
Control	ΔE_{Na}: −2.9	−43.1	242.5	−4.3	27.2
20 K	ΔE_K: 36.7	−30.0	145.1	−2.4	25.2
ΔE		13.1		1.9	
R exp/R contr			0.60		0.93
Control	ΔE: −10.0	−45.7	184.3	−5.9	22.9
50 K	ΔE_K: 61.0	−18.8	61.2	−3.3	18.3
ΔE		26.9		2.6	
R exp/R contr			0.33		0.80
Control	ΔE_{Na}: −28.9	−44.8	188.3	−4.6	31.9
100 K	ΔE_K: 79.4	−5.3	62.6	−1.3	16.5
ΔE		39.4		3.4	
R exp/R contr			0.33		0.52
Low chloride					
Control		−35.7	175.8	−4.8	25.8
IE	ΔE_{Cl}: 91.0	−12.3	244.8	−2.4	40.1
ΔE		23.4		2.4	
R exp/R contr			1.39		1.55

Control values are obtained by assuming a negligible loop current and $R_C = 778.5$ MΩ and $R_i = 58.3$ MΩ (Table 1). Experimental values are calculated by assuming that the emf (E_C) and resistance (R_C) across the canalicular membrane and the cell coupling resistance (R_i) remain unchanged during the ionic shift.

brane potential is shown in Fig. 7, which also demonstrates that the cellular input resistance did not change immediately after K^+ readmission (control value 106.0 ± 16.8 MΩ, n = 8). Two recordings were obtained for an extended period of time (Fig. 7) and indicated that the cellular input resistance progressively decreased after K^+ readmission, apparently due to the reaccumulation of internal K^+. K^+ readmission consistently resulted in a small but significant hyperpolarization of the luminal potential (from −1.9 to −3.2 ± 0.4 mV, n = 8) with no apparent changes of input resistance.

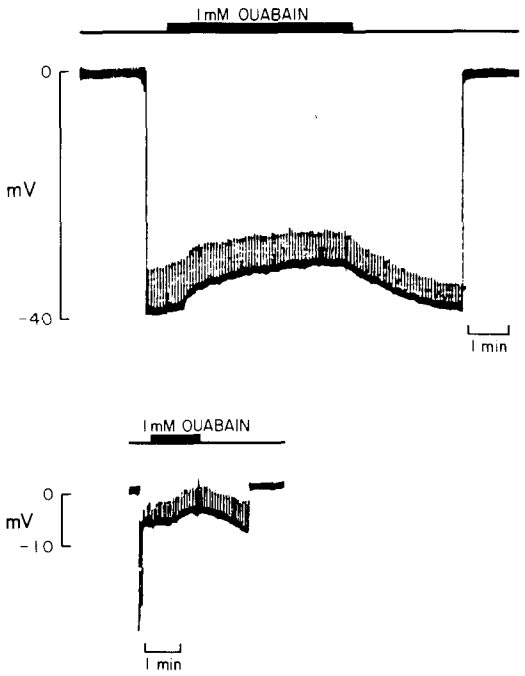

Fig. 6. Effect of 1 mM ouabain on intracellular (upper trace) and intraluminal (lower trace) electrical potential. Note the initial step depolarization of the intracellular potential reflecting inhibition of the electrogenic Na pump. Both cellular and luminal depolarizations were reversible upon removal of ouabain. No consistent changes of input resistances were obtained

Discussion

The findings in the present study provide a detailed analysis of the basic electrophysiologic properties of the IRHC. Measurement of the intracellular electric potential (Tables 1 and 3) are comparable to those obtained in an earlier study (Graf et al., 1984).

Results of the circuit analysis (Fig. 2 and Table 1) reveal that the cells are electrically coupled as in intact tissue (Penn, 1966; Graf & Petersen, 1978; Meyer, Yancey & Revel, 1981; Spray et al., 1986). The resistances of the tight junctions that seal the canalicular lumen from the bathing media are comparable to those obtained in other leaky epithelia (Claude, 1978) and allow rapid ion equilibration between these two compartments.

Measurements of intracellular ion concentrations (Na^+, K^+ and Cl^-) are consistent with values obtained from analysis of the whole organ and indicate that Cl^- is passively distributed, whereas transmembrane Na^+ and K^+ concentration gradients are maintained by the pump activity of Na^+K^+-ATPase. This pump is located at the basolateral membrane (Blitzer & Boyer, 1978; Latham & Kashgarian, 1979) and is electrogenic (Graf & Petersen, 1978), but pump current contributes little to the generation of the negative canalicular luminal potential. This luminal potential appears to result from a Donnan distribution, whereas the intracellular potential is mainly determined by ion gradients and ion conductances of the sinusoidal-basolateral membrane.

This study also attempts to provide a quantitative assessment of these electrical properties in IRHC. Since these quantitative conclusions are inherently dependent on the accuracy of the measurements, the possibility of methodological artifacts must first be considered.

Electrophysiological studies on cells isolated from parenchymal organs have frequently revealed lower membrane potentials than those obtained in the intact organ. This phenomenon has been attributed to the possibility that membrane leaks, induced by micropuncture, more effectively shunt the membrane potential the higher the total cell membrane resistance. This may be a particular problem when large electrodes are used in small single cells (Douglas & Taraskevich, 1985; Hosoi & Slayman, 1985; Trifaro & Poisner, 1985; Oberleithner, Schmidt & Dietl, 1986). In intact liver tissue the input resistance is very low due to extensive current flow into neighboring cells through low resistance intracellular communications (e.g. 0.6 MΩ in mouse liver) (Graf & Petersen, 1978). Hence, the cell membrane potential of the impaled cell in the intact organ may be held to values close to normal by its intact neighbors. Impalement damage was minimized by using small tip-size electrodes. When compared with potential measurements from intact tissue, our values are in the lower range of most of those reported except for those in Table 3 where single small tip-size electrodes were used. Membrane potentials obtained in vivo ranged from −31 to −46 mV (Kernan & MacDermott, 1980; Meyer et al., 1981; Fitz & Scharschmidt, 1985) and in the

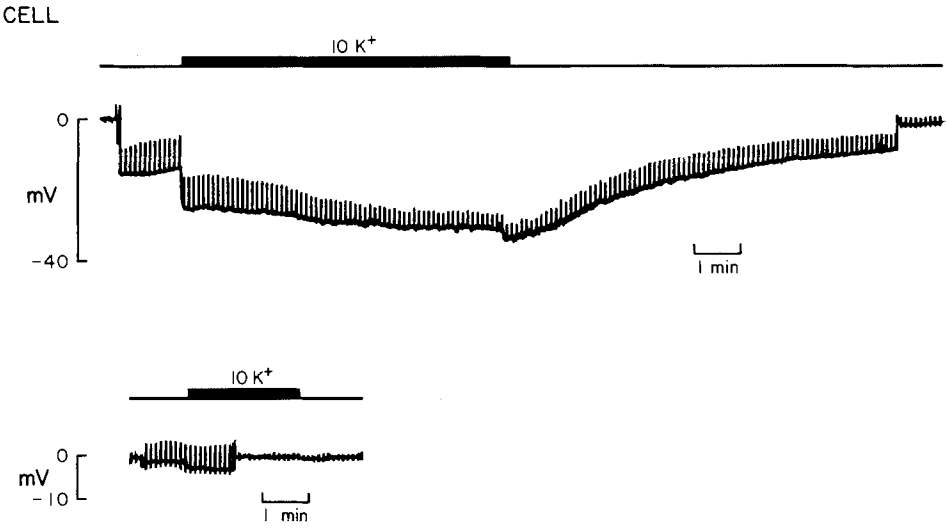

Fig. 7. Effect of K^+ readmission on cellular (upper trace) and luminal (lower trace) electric potentials. Cells were preincubated in K-free medium in order to decrease internal K^+ concentration and increase internal Na^+ concentration by inhibition of the Na^+ pump. Readmission of K^+ to the external medium causes pump activation. Cell hyperpolarization occurs despite a reduction of transmembrane E_K showing the electrogenicity of the pump. The decrease of the amplitude of electrotonic potential (cellular input resistance) is consistent with reaccumulation of internal K^+ and a high membrane K permeability. A transient hyperpolarization followed by a slow reduction of the cell membrane potential is seen after subsequent omission of external K^+. These latter effects are also consistent with a high membrane K permeability and loss of internal K^+. The lower trace shows that K^+ readmission has only a small hyperpolarizing effect on the luminal potential. Perfusion was shifted to K^+-free medium after the electrode was withdrawn from the lumen, revealing no potential deflection. Electrode artifacts accounting for the small luminal potential change therefore appear unlikely

perfused liver from −29 to −34 mV (Claret et al., 1970; Wondergem & Harder, 1980; Cohen et al., 1982). A second criterion for impalement quality is the value of the membrane resistance which was 3 kΩ cm² in the present study ($1/g_S$–Table 1). This value compares with a mean specific membrane resistance of 9.1 kΩ cm² in intact rat liver and 5.1 kΩ cm² in the mouse liver segment (Graf & Petersen, 1978; Meyer et al., 1981). Only preliminary data on input resistances of single cells determined by whole cell patch-clamp recordings are available: guinea pig, 560 MΩ (Capiod & Ogden, 1985) and rat, ~280 MΩ (M. Hunter, *unpublished data*). These data compare to ~150 to 260 MΩ (R_S in Tables 1 and 4) obtained in this study. Thus, on the basis of these comparisons, membrane potentials as well as resistances measured in the IRHC are below values obtained in intact tissue or with patch-clamp electrodes. This observation applies particularly to measurements obtained with two electrodes or with double-barreled electrodes, where leak resistances may have been induced by the impalement. Thus the more negative cellular potential measurements (Table 3) reflect more accurately the true intracellular membrane potential. This conclusion is further supported by measurements of intracellular chloride activities. Immediately after impalement intracellular chloride activities corresponds to an E_{Cl} of −44.3 mV. Intracellular chloride concentration ($[Cl^-]_i$) rose after impalement to values where $E_{Cl} \sim V_S$ (Fig. 4). This observation suggests that Cl^- is passively distributed according to the membrane potential, a notion also supported by the finding that $[Cl^-]_i$ decreased by artificial cell hyperpolarization (current clamp) and increased by depolarization (Fig. 4). Therefore, determination of E_{Cl} immediately after impalement would appear to give a better approximation of the true membrane potential.

Another possible source of artifacts concerned with microelectrode impalements of small cells is electrolyte leakage from the electrode tip (Blatt & Slayman, 1983). This problem became evident in a few experiments in which we attempted to use electrodes with tip resistances of less than 100 MΩ.

Intracellular ion concentrations have been determined in various hepatic preparations using a number of techniques (Claret & Mazet, 1972; Graf & Peterlik, 1975; Graf & Petersen, 1978; Kernan & MacDermott, 1980; Scharschmidt & Stephens, 1981; Beck et al., 1982; Van Dyke & Scharschmidt, 1983). Values for intracellular concentrations of Cl^- ranged from 21.0 to 33.0 mM; for Na^+ from 6.5 to 16.7 mM and for K^+ from 113.0 to 169.0 mM. There is fairly good agreement between these measurements and those obtained in IRHC (Table 2). Estimates of conductive ion fluxes and membrane ion

conductances in liver cells in other studies have been based on several different techniques and experimental models. In particular, unidirectional ion fluxes have been determined in the perfused rat liver (Claret, 1979; Graf & Peterlik, 1975), electrophysiological measurements of transference numbers have been performed in different preparations of rat and mouse liver (Claret, 1979; Graf & Petersen, 1978) and net fluxes have been determined in isolated rat hepatocytes (Scharschmidt & Stephens, 1981; Van Dyke & Scharschmidt, 1983). It is quite difficult to compare these data to those obtained in the IRHC for both theoretical and practical reasons. Unidirectional ion fluxes have been measured in these other studies using isotopes to determine the influx or efflux component at quasi steady-state conditions, whereas net fluxes are obtained by disturbing this equilibrium by drastically reducing either one of the two components. In addition, both measurements may include nonconductive electrically silent fluxes. Data are also reported using different dimensions so that their interconversion relies on assumption of parameters such as number of cells/unit tissue weight, volume/mg cell protein, or membrane area per cell. Using conversion factors given in these reports and morphometric data (Weibel et al., 1969) a range of estimates of fluxes (given as $\times 10^{-18}$ moles/cell/sec) can be calculated for a single hepatocyte: Na^+: 118–267, K^+: 109–333, Cl^-: 133–592. These figures may be compared to data obtained in IRHC by equations relating conductive fluxes for individual ions (J_i) current (I_i), ion conductance (g_i), permeability (P_i), ion concentrations on both sides of the membrane ($[i]_i$, $[i]_o$), chemical potential gradients (E_i) and membrane potential (V_m), e.g.: $I_K = J_K F = g_K(V_m - E_K) = I_K = P_K F^2 V_m([K^+]_o - [K^+]_i \exp - V_m F/RT)/RT(1 - \exp V_m F/RT)$ (Hodgkin & Katz, 1949). Relevant data to obtain these estimates for the sinusoidal cell membrane of IRHC are given in Tables 1 to 4. Transference numbers ($t_i = g_i/g_s$) are calculated by $\Delta E_S = \Sigma t_i \cdot \Delta E_i$ for data given in Tables 1 and 3. Values obtained are: $t_{Na} = 0.056$, $t_K = 0.360 - 0.517$ (depending upon the concentration of K^+ used in the ion substitution which ranged from 20 to 100 mM) and $t_{Cl} = 0.257$. From these the following conductive steady-state net fluxes of a single cell are calculated for a membrane potential (V_S) of −40 mV (again $\times 10^{-18}$ moles/cell/sec): $J_{Na(in)} = 377$, $J_{K(out)} = 1304$ to 1874, $J_{Cl(in)} = 452$. For $V_S = -44.3$, $J_{Na} = 386$, $J_K = 950$ to 1365 and $J_{Cl} = 0$ (electrochemical equilibrium). Ion permeabilities obtained from the right-hand term of the Hodgkin and Katz (1949) equation are ($\times 10^{-7}$ cm/sec) $P_{Na} = 0.6\, P_K = 12.7$ to 18.2, $P_{Cl} = 4.6$. This permeability sequence is also reflected by the dependence of membrane ion conductance on external ion concentration. Thus the membrane conductance increases when external K^+ is increased, and a reduction in membrane conductance is observed when external Cl^- is reduced, which is larger than noted upon reducing external Na^+. In summary, the observations on membrane potential, membrane resistances, intracellular ion concentrations and membrane ion conductances in IRHC are in reasonable agreement with studies performed in intact liver tissues. As in intact liver, the intracellular potential is determined largely by the transmembrane K^+ gradient and therefore modulation of the K^+ conductance is likely to be the major regulatory mechanism for altering intracellular potential.

This study also gives an estimate of the conductance of the tight junction per unit length (37 μS/cm). Compared to data obtained in a large number of other epithelia (Claude, 1978) liver tight junctions are as leaky as those of the proximal tubule or small intestine, epithelia capable of isoosmotic transepithelial fluid transport. This notion is consistent with earlier observations in intact liver, which showed very rapid dissipation of ion gradients established experimentally between vascular space and bile, rapid isotope equilibration between these compartments and penetration of tight junctions by ionic lanthanum (Graf & Peterlik, 1975; Layden, Elias & Boyer, 1978; Van Dyke, Stephens & Scharschmidt, 1982; Anwer & Hegner, 1983; Graf, 1983). In contrast, Ruthenium red, an electron-dense marker of 551 Daltons, is excluded from penetration into the canalicular space in cultured hepatocytes (Wanson et al., 1977) and also in the IRHC model (Boyer et al., 1985). Measurements of diffusion potential between canalicular lumen and bath of the IRHC during ion substitutions in the bathing media revealed only small changes of the luminal electric potential (Table 3). It is therefore assumed that the paracellular pathway exhibits little ion selectivity. Since $E_T = t_i \Delta E_i + t_{sub} \Delta E_{sub}$, the small change in luminal potential actually indicates that there is permeation of the ion substitute. A calculation of transference numbers is therefore not feasible since the chemical potential of the ion substitute (ΔE_{sub}) is infinite. Qualitatively high Na^+ and Cl^- conductances of the tight junctions are also suggested by the observation that R_T increases when external Na^+ or Cl^- are replaced, although part of this change could be due to shrinkage of the canalicular lumen and the lower mobilities of the substituting ions within the lateral intercellular space.

Cell coupling by low resistance intercellular communications has been described in intact liver (Penn, 1966; Graf & Petersen, 1978; Meyer et al., 1981) and also recently in isolated hepatocyte couplets (Reverdin & Weingart, 1986; Spray et al.,

1986). We obtained a mean intercellular resistance of 58 MΩ, but it was noted that there was a fairly large variability in the extent of cell-to-cell coupling. From the resistivity for intercellular current spread measured in intact tissue by cable analysis, single cell-to-cell resistances are calculated to be in the order of 1–2 MΩ only (Graf & Petersen, 1978; Meyer et al., 1981). Our data therefore indicate that the gap junction area or the number of connexons between IRHC is considerably smaller than in intact tissue; nonetheless, gap junctions do exist between the two cells as demonstrated by freeze-fracture studies (*unpublished observations*).

Electrogenic sodium pumping has been demonstrated previously by K^+ readmission in mouse and rat liver tissue (Graf, 1976; Graf & Petersen, 1974). In IRHC in the present study we showed that inhibition of (Na^+-K^+)-ATPase by K^+ deprivation leads to an increase of intracellular Na^+ and a loss of intracellular K^+. Pump activation by K^+ readmission resulted in the rapid hyperpolarization of the cells together with a recovery of internal K^+ at an approximate rate of 9.4 mM/min. Using resistance values in Table 1 and the equivalent circuit in Fig. 1 and locating the pump to the sinusoidal liver cell membrane, the hyperpolarization by 8.7 mV would be produced by a pump current (I_p) of 67 pA/cell whereas the rate of K^+ recovery is approximately 1.6×10^{-15} moles/sec, a value in fairly good agreement with a 3 Na^+/2K^+ coupling ratio of the pump transferring one charge per cycle ($I_p/F = 0.7 \times 10^{-15}$ moles/sec). Given the resistances reported in Table 1, the fraction of pump current reentering the cell through R_T and R_C would cause a hyperpolarization of V_B and V_C by −0.5 and −8.2 mV, respectively. The hyperpolarization of V_B by −1.3 mV actually observed during K^+ readmission would indicate that the ratio R_T/R_C is 0.07, which is in reasonable agreement with the ratio of 0.03 calculated from the data obtained with two microelectrodes reported in Table 1.

Ouabain led to a small depolarization of the intracellular potential by 2.9 mV. This would indicate that the Na^+ pump contributes little to this potential under control conditions and its effect on the luminal potential would be <0.2 mV, a value that would be below the level of detection.

Similar to this small hyperpolarizing effect of the Na^+ pump in rat hepatocytes, other electrogenic transport processes such as Na^+-coupled amino acid transport would cause only small membrane potential changes of 0.13 mV/pA.

According to the equivalent circuit shown in Fig. 1, two sources of the canalicular lumen negative potential V_B may be considered. V_B could be the result of current flow through R_T. Alternatively, V_B could be the result of a diffusion potential establishing the emf E_T with no or little current flow in the loop $R_T \rightarrow R_C \rightarrow R_S$. Two considerations make the latter possibility appear more likely: (i) Given the resistance values reported in Table 1, a basolateral (sinusoidal) pump would have to produce a current of >500 pA to establish a luminal potential of −4.3 mV. This would correspond to an ion flux of $>5 \times 10^{-15}$ moles/sec, a value one order of magnitude higher than expected from our estimates on electrogenic ion fluxes. (ii) The secretory rate of IRHC is approximately 3.2×10^{-15} liter/couplet/min (Gautam, Scaramuzza & Boyer, 1986). Assuming isoosmotic fluid transport, this is equivalent to the secretion of monovalent salts at a rate of approximately 8×10^{-18} moles/sec. This could be accomplished by electrogenic secretion of anions across the canalicular cell membrane, whereas cations could enter the lumen through the tight junction thus producing a loop current of 0.4 pA/cell. This current from two cells flowing through R_T would produce an intraluminal potential of −20 μV only. Thus we conclude that loop current is an insignificant source of the luminal potential. Therefore it seems likely that V_B is mainly a diffusion potential, set up by the secretion of impermeant anions across the canalicular membrane. If this conclusion is correct, the luminal space should contain impermeant anions, at a concentration of approx 50 mM, a value about twice as high as the "cation-anion gap" of electrolytes present in bile collected distally from bile ducts in the intact liver (Klos, Paumgartner & Reichen, 1979; Graf, 1983).

In conclusion, classical techniques of epithelial electrophysiology have been applied in order to determine the basic electrical characteristics of the isolated rat hepatocyte couplet system. In a modified circuit analysis we obtained estimates of the transepithelial potential and resistance, the resistances for paracellular (tight junction) and transcellular current flow, the latter including the luminal and basolateral membrane resistance, and estimates of the transcellular voltage profile. The data show a canalicular lumen negative potential of −4 mV, a low resistance and poor ion selectivity of the paracellular pathway, electrical properties also reported in other leaky epithelia. The luminal cell membrane resistance is >5 times higher than that of the basolateral membrane. Intracellular electrolyte activities and electric potential found for IRHC, are similar to data obtained in intact liver. The cell potential is mainly determined by ion conductances of the basolateral membrane. The basolateral (Na^+-K^+)-ATPase is electrogenic, hyperpolarizing the cell interior upon activation. Pump activation or pump inhibition has little influence on the luminal poten-

tial. This canalicular lumen potential may result from unequal concentrations of permeant electrolytes on both sides of the tight junction barrier, probably in accordance with a Donnan distribution. In this *in vitro* system, the liver cells remain electrically coupled as in intact tissue.

These experiments were performed at Yale in the laboratory of Dr. Gerhard Giebisch, to whom we express our gratitude. We are also grateful to Dawn Scaramuzza and Pamela Missal for skilled technical assistance. Supported by N.I.H. AM/HL 17433, AM 36854 and the Hepatocyte Isolation Core from the Liver Center AM 34989. Dr. Jürg Graf received support from the Austrian National Bank and the Hochschule jubiläums Stiftung der Gemeinde Wien. Dr. Graf wishes to thank G.E. Graf for valuable assistance in computer calculations.

References

Anwer, M.S., Hegner, D. 1983. Role of inorganic electrolytes in bile acid-independent canalicular bile formation. *Am. J. Physiol.* **244:**116–124

Beck, F., Dörge, A., Mason, J., Rick, R., Thurau, K. 1982. Element concentrations of renal and hepatic cells under potassium depletion. *Kidney Int.* **22:**250–256

Blatt, M.R., Slayman, C.L. 1983. KCl leakage from microelectrodes and its impact on the membrane parameters of a non-excitable cell. *J. Membrane Biol.* **72:**223–234

Blitzer, B.L., Boyer, J.L. 1978. Cytochemical localization of Na^+, K^+-ATPase in the rat hepatocyte. *J. Clin. Invest.* **62:**1104–1108

Blitzer, B.L., Ratoosh, S.L., Donovan, C.B., Boyer, J.L. 1982. Effects of inhibitors of Na^+-coupled ion transport on bile acid uptake by isolated rat hepatocytes. *Am. J. Physiol.* **243:***G*48–*G*53

Boulpaep, E.L., Sackin, H. 1979. Equivalent electrical circuit analysis and rheogenic pumps in epithelia. *Fed. Proc.* **38:**2030–2036

Boyer, J.L., Ng, O.-C., Gautam, A. 1985. Formation of canalicular spaces in isolated rat hepatocyte couplets. *Trans. Assoc. Am. Phys.* **98:**21–29

Capiod, T., Ogden, D. 1985. Noise analysis of α-adrenergic activated K-conductance in isolated guinea pig hepatocytes. *J. Physiol. (London)* **369:**107*P*

Claret, M. 1979. Transport of ions in liver cells. *In:* Membrane Transport in Biology. G. Giebisch, D.C. Tosteson, and H.H. Ussing, editors. Vol. 4, pp. 899–920. Springer-Verlag, Berlin–Heidelberg–New York

Claret, M., Coraboeuf, E., Favier, M.P. 1970. Effect of ion concentration changes on membrane potential of perfused rat liver. *Arch. Int. Physiol. Biochim.* **78:**531–545

Claret, M., Mazet, J.L. 1972. Ionic fluxes and permeabilities of cell membranes in rat liver. *J. Physiol. (London)* **223:**279–295

Claude, P. 1978. Morphological factors influencing transepithelial permeability: A model for the resistance of the zonula occludens. *J. Membrane Biol.* **39:**219–232

Cohen, R.D., Henderson, R.M., Iles, R.A., Smith, J.A. 1982. Metabolic inter-relationships of intracellular pH measured by double-barrelled micro-electrodes in perfused rat liver. *J. Physiol. (London)* **330:**69–80

Douglas, W.W., Taraskevich, P.S. 1985. The electrophysiology of the adenohypophyseal cells. *In:* Electrophysiology of the Secretory Cell. A.M. Poisner and J.M. Trifaro, editors. pp. 63–92. Elsevier, Amsterdam

Fitz, J.G., Scharschmidt, B.F. 1985. Regulation of transmembrane electrical potential (E_m) of rat hepatocytes *in situ*. (*Abstr.*) *Hepatology* **5:**1011

Gautam, A., Scaramuzza, D., Boyer, J.L. 1986. Quantitative assessment of primary canalicular secretion in isolated rat hepatocyte couplets (IRHC) by optical planimetry. (Abstr.) *Gastroenterology* **90:**1727

Graf, J. 1976. Sodium pumping and bile secretion. *In:* The Liver: Quantitative Agents of Structure and Function. R. Presig, J. Bircher, and G. Paumgartner, editors. pp. 370–385. Edito Cantor, Aulendorf, W. Germany

Graf, J. 1983. Canalicular bile salt independent bile formation: Concepts and clues for electrolyte transport in rat liver. *Am. J. Physiol.* **244:***G*233–*G*246

Graf, J., Gautam, A., Boyer, J.L. 1984. Isolated rat hepatocyte couplets: A primary secretory unit for electrophysiologic studies of bile secretory function. *Proc. Natl. Acad. Sci. USA* **81:**6516–6520

Graf, J., Giebisch, G. 1979. Intracellular sodium activity and sodium transport in *Necturus* gallbladder epithelium. *J. Membrane Biol.* **47:**327–355

Graf, J., Peterlik, M. 1975. Mechanisms of transport of inorganic ions into bile. *In:* The Hepatobiliary System-Fundamental and Pathological Mechanisms. W. Taylor, editor. pp. 43–58. Plenum, New York

Graf, J., Petersen, O.H. 1974. Electrogenic sodium pump in mouse liver parenchymal cells. *Proc. R. Soc. London B* **187:**363–367

Graf, J., Petersen, O.H. 1978. Cell membrane potential and resistance in liver. *J. Physiol. (London)* **284:**105–126

Henderson, R.M., Graf, J., Boyer, J.L. 1987. Na-H exchange regulates intracellular pH in isolated rat hepatocyte couplets. *Am. J. Physiol.* **252:**G109–G113

Hodgkin, A.L., Katz, B. 1949. The effect of sodium ions on the electrical activity of the giant axon of the squid. *J. Physiol. (London)* **108:**37–77

Hosoi, S., Slayman, C.L. 1985. Membrane voltage, resistance, and channel switching in isolated mouse fibroblasts (L cells): A patch electrode analysis. *J. Physiol. (London)* **367:**267–290

Kernan, R.P., MacDermott, M. 1980. Measurement of potassium and chloride activities in liver cells and in extensor digitorum longus muscle fibres of anaesthetised rats in situ. (*abstr.*) *Proc. Int. Union. Physiol. Sci.* **14:**510

Klos, C., Paumgartner, G., Reichen, J. 1979. Cation anion gap and choleretic properties of rat bile. *Am. J. Physiol.* **236:***E*434–*E*441

Latham, P.S., Kashgarian, M. 1979. The ultrastructural localization of transport ATPase in the rat liver at non-bile canalicular plasma membrane. *Gastroenterology* **76:**988–996

Layden, T.J., Elias, E., Boyer, J.L. 1978. Bile formation in the rat. *J. Clin. Invest.* **62:**1375–1385

Loewenstein, W.R. 1979. Functional intercellular communication and the control of growth. *Biochim. Biophys. Acta* **560:**1–65

Meyer, D.J., Yancey, S.B., Revel, J.P. 1981. Intercellular communication in normal and regenerating rat liver: A quantitative analysis. *J. Cell Biol.* **91:**505–523

Oberleithner, H., Schmidt, B., Dietl, P. 1986. Fusion of renal

epithelial cells: A novel model for studying cellular mechanisms of ion transport. *Proc. Natl. Acad. Sci. USA* **83:**3547–3551

Penn, R.D. 1966. Ionic communications between liver cells. *J. Cell Biol.* **29:**171–174

Reverdin, E., Weingart, R. 1986. Electrical coupling studied in cell pairs isolated from adult rat liver. *J. Physiol. (London)* **372:**46P

Sackin, H., Boulpaep, E.L. 1983. Rheogenic transport in the renal proximal tubule. *J. Gen. Physiol.* **82:**819–851

Scharschmidt, B.F., Stephens, J.E. 1981. Transport of sodium, chloride, and taurocholate by cultured rat hepatocytes. *Proc. Natl. Acad. Sci USA* **78:**986–990

Seglen, P.O. 1976. Preparation of isolated rat liver cells. *Methods Cell. Biol.* **13:**29–83

Spray, D.C., Ginzberg, R.D., Morales, E.A., Gatmaitan, Z., Arias, I.M. 1986. Electrophysiological properties of gap junctions between dissociated pairs of rat hepatocytes. *J. Cell Biol.* **103:**135–144

Thomas, R.C., Cohen, C.J. 1981. A liquid ion-exchanger alternative to KCl for filling intracellular reference microelectrodes. *Pfluegers Arch.* **390:**96–98

Trifaro, J.M., Poisner, A.M. 1985. Electrophysiological properties of secretory cells: On an overview. *In:* The Electrophysiology of the Secretory Cell. A.M. Poisner and J.M. Trifaro, editors. pp. 269–302. Elsevier, Amsterdam

Van Dyke, R.W., Scharschmidt, B.F. 1983. (Na,K)-ATPase mediated cation pumping in cultured rat hepatocytes. *J. Biol. Chem.* **258:**12,912–12,919

Van Dyke, R.W., Stephens, J.E., Scharschmidt, B.F. 1982. Effect of ion substitution on bile formation by the isolated perfused rat liver. *J. Clin. Invest.* **70:**505–517

Wanson, J.-C., Drochmans, P., Mosselmans, R., Rouveaux, M.-F. 1977. Adult rat hepatocytes in primary monolayer culture. *J. Cell Biol.* **74:**858–877

Weibel, E.R., Staubli, W., Gnagi, H.R., Hess, F.A. 1969. Correlated morphometric and biochemical studies on the rat liver. *J. Cell Biol.* **42:**68–91

Wondergem, R., Harder, D.R., 1980. Membrane potential measurements during rat liver regeneration. *J. Cell. Physiol.* **102:**193–197

Received 23 July 1986; revised 24 November 1986